ACS APPLIED MATERIALS & INTERFACES

Letter

www.acsami.org

Heating-Rate-Induced Porous α-Fe_2O_3 with Controllable Pore Size and Crystallinity Grown on Graphene for Supercapacitors

Shuhua Yang, Xuefeng Song,* Peng Zhang, and Lian Gao*

State Key Laboratory for Metallic Matrix Composite Materials, School of Materials Science and Engineering, Shanghai Jiao Tong University, Shanghai 200240, China

Supporting Information

ABSTRACT: Porous α-Fe_2O_3/graphene composites (S-PIGCs) have been synthesized by a simple hydrothermal method combined with a slow annealing route. The S-PIGCs as a supercapacitors electrode material exhibit an ultrahigh specific capacitance of 343.7 F g^{-1} at a current density of 3 A g^{-1}, good rate capability, and excellent cycling stability. The enhanced electrochemical performances are attributed to the combined contribution from the optimally architecture of the porous α-Fe_2O_3, as a result of a slow annealing, and the extraordinary electrical conductivity of the graphene sheets.

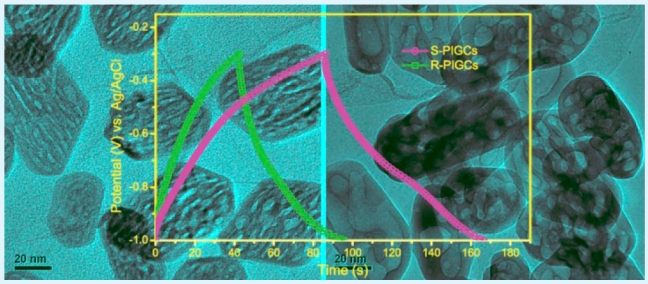

KEYWORDS: *heating-rate-induced porous α-Fe_2O_3, pore size, crystallinity, supercapacitors*

Supercapacitors with long cycle life and short charging time are one of desirable energy storage devices.[1−3] α-Fe_2O_3 is a promising material for supercapacitors because of its good pseudocapacitive feature, natural abundance, and environmental harmlessness.[4−6] Nevertheless, its practical application is severely hindered by the poor electrical conductivity. Graphene, a single layer of two-dimensional carbon atoms with extraordinary electrical conductivity, has attracted unparalleled attention as an ideal conducting support to modify transition metal oxides in supercapacitors.[7] For example, Lee et al. fabricated α-Fe_2O_3 nanotubes anchored on reduced graphene oxide, which exhibited excellent specific capacitance (216 F g^{-1}) and cycling life.[5] Very recently, we also reported a novel α-Fe_2O_3 mesocrystals/graphene nanohybrid used as a supercapacitor electrode, which exhibited high specific capacitance (306 F g^{-1}).[6] Although the compositing of graphene offers an effective processing protocol to improve the electrochemical performances of α-Fe_2O_3, exploiting the feature of α-Fe_2O_3 is required in order to enhance both the kinetics and the capacitances of the α-Fe_2O_3 based electrodes. Research has generally been focused on the design of diverse architecture of the constituent α-Fe_2O_3 on graphene, such as nanotubes or mesocrystals. The controlled microstructure and crystallinity of α-Fe_2O_3 nanoparticles on graphene has gained less attention. Achieving a precise control is particularly challenging in the composites consisting of graphene and transition metal oxides because the combination of the graphene makes the synthesis of the inorganic oxides with specific architectures more complicated.[8]

Transition metal oxides with porous nanostructures have been found to be an effective alternate to improve the charge storage of supercapacitors because of their high surface area, short electron and ion transport pathway, and enhanced interaction with the electrolyte ions.[9−11] Numerous research efforts for preparation of porous inorganic materials with various structure have been developed, especially by soft-templating and hard-templating method.[12] However, the block copolymer derived metal oxides only have amorphous frameworks, whereas porous metal oxides prepared by the hard-templating method have been proven to be very difficult to control the mesopore diameters.[13,14] Although some porous metal oxides have been synthesized by thermal treatment, their pore sizes and crystallinity are uncontrollable.[15] Therefore, developing practical methods for the preparation of porous metal oxides with well-controlled pore sizes and crystallinity, accompanying with high capacitance, still remains a challenge. In addition, it is highly desirable to fabricate such architecture for supercapacitors to overcome the diffusion limitation, improve the surface area, and optimize the crystallite size effect.

Herein, we report a simple hydrothermal method combined with a slow annealing route to prepare porous α-Fe_2O_3-graphene composites (S-PIGCs). The pore size and crystallinity can be controlled by varying the heating rate. As a control experiment, the other PIGCs was also prepared by a similar method but using a rapid annealing process, designated as R-PIGCs. The S-PIGCs exhibit an ultrahigh specific capacitance, good rate capability, and excellent cycling stability in a mild aqueous electrolyte. As far as we know, this is the highest capacitance ever reported for Fe_2O_3 nanostructures (see Table S1 in the Supporting Information),[4−6,16] which is attributed to the controllable pore size and crystallinity of the porous α-

Received: November 11, 2014
Accepted: December 23, 2014
Published: December 23, 2014

DOI: 10.1021/am507910f
ACS Appl. Mater. Interfaces 2015, 7, 75−79

Fe_2O_3, as well as the extraordinary electrical conductivity of the graphene sheets.

X-ray diffraction (XRD) pattern of the composites (RGO-FeOOH) before annealing corresponds well to that of goethite (FeOOH) (Figure 1), signifying the successful growth of FeOOH on graphene under hydrothermal conditions. After annealing, all peaks of the XRD pattern of S-PIGCs and R-PIGCs can be indexed to the rhombohedral phase of hematite (α-Fe_2O_3, JCPDS No. 33−0664) (Figure 1). It is clear that the S-PIGCs show lower crystallinity compared to R-PIGCs. On the basis of the Scherer equation, the mean crystallite sizes of α-Fe_2O_3 are estimated to be 15.3 and 33.2 nm for S-PIGCs and R-PIGCs, respectively, which are larger than that of α-Fe_2O_3 in α-Fe_2O_3 mesocrystals/graphene nanohybrid (11 nm) reported by our group.[6] This indicates that the annealing route can significantly improve the crystallinity of α-Fe_2O_3 and tune the crystallinity of α-Fe_2O_3 through changing the heating rate. The control over the crystallinity is highly desired, because it is well-established that the electrode materials with an appropriate crystallite size could show higher capacitances than that of either amorphous or crystalline material, especially when possessing the porous structure.[1,17,18] No peaks of graphene sheets are detected, suggesting that the graphene sheets are disorderly stacked with a low degree of graphitization because the porous α-Fe_2O_3 on the graphene sheets prevent the graphene sheets from restacking.[6,19] From the TEM image, the as-made FeOOH nanoparticles with short rodlike shape are uniformly dispersed on the graphene sheets under hydro-

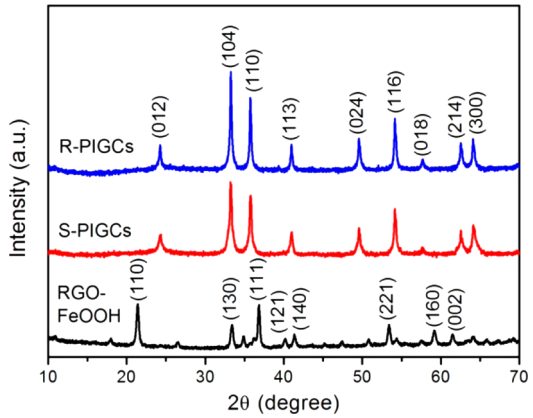

Figure 1. XRD patterns of RGO-FeOOH composites, R-PIGCs, and S-PIGCs.

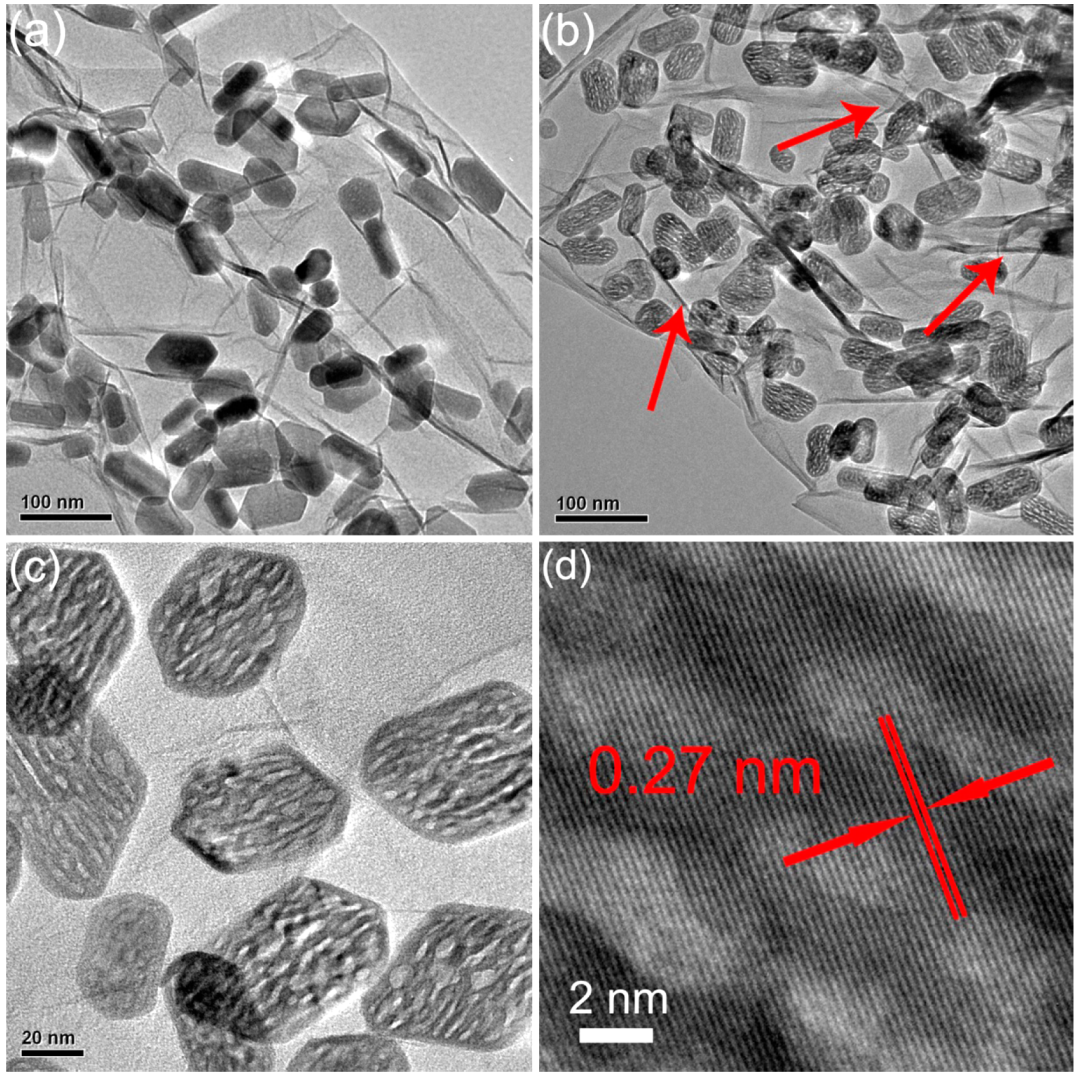

Figure 2. (a) TEM image of RGO-FeOOH composites, (b, c) TEM images of S-PIGCs, (d) HRTEM image of porous α-Fe_2O_3.

DOI: 10.1021/am507910f
ACS Appl. Mater. Interfaces 2015, 7, 75−79

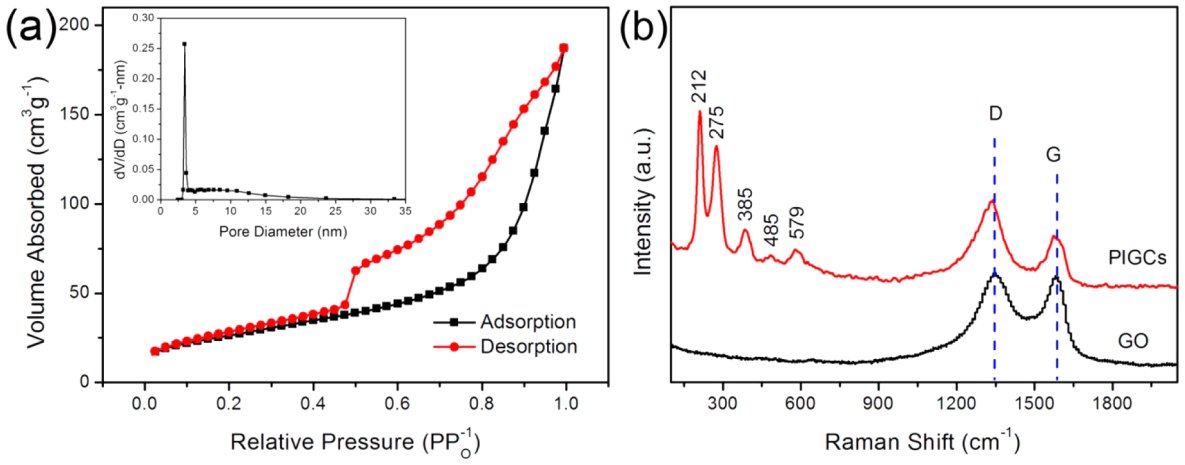

Figure 3. (a) Nitrogen adsorption and desorption isotherms and the corresponding pore size distribution curve of S-PIGCs. (b) Raman spectra of S-PIGCs and GO.

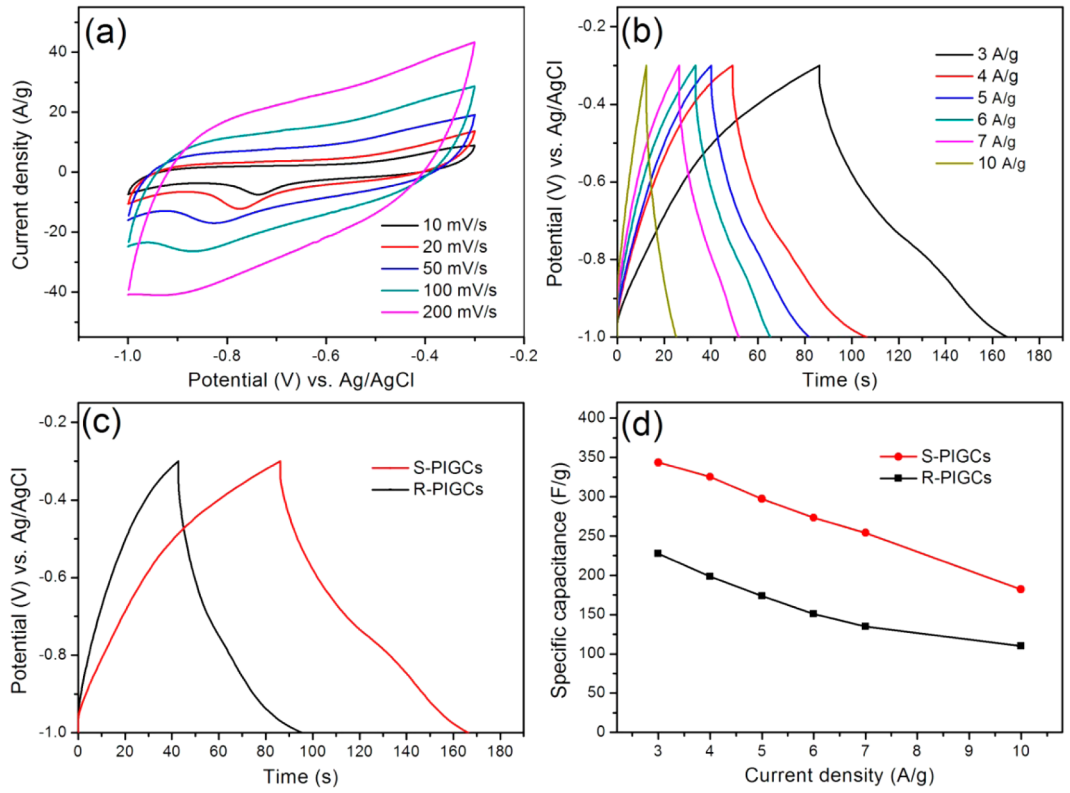

Figure 4. (a) CV curves of S-PIGCs at different scan rates, (b) CD curves of S-PIGCs at different current densities, (c) CD curves for S-PIGCs and R-PIGCs at a current density of 3 A g^{-1}, (d) Variation of specific capacitance against current density for S-PIGCs and R-PIGCs.

thermal treatment (Figure 2a). After annealing, the original rodlike shape and the dispersion of the nanoparticles on the graphene sheets were well-preserved, whereas the FeOOH nanoparticles in situ transformed to porous α-Fe_2O_3 nanoparticles along with an improved crystallinity (Figure 2b and Figure S1 in the Supporting Information). The FFT pattern of α-Fe_2O_3 nanoparticles also confirms that S-PIGCs have lower crystallinity than R-PIGCs (see Figure S2 in the Supporting Information). Additionally, the graphene sheets have numerous wrinkles and folds (as indicated by the red arrows in Figure 2b), which provide more reactive sites and functionalities for tuning the reaction barrier and reaction energetics of graphene.[20,21] Further information about the porous α-Fe_2O_3 nanoparticles can be obtained from a zoom-in TEM image (Figure 2c). It is confirmed that the α-Fe_2O_3 nanoparticles possess slit-like pores open to the outer surface with the pore width of 3−4 nm. From the high-resolution TEM (HRTEM) image (Figure 2d), the fringe spacing of about 0.27 nm corresponds to the value of the (104) plane of α-Fe_2O_3 phase, which is in agreement with the powder XRD result. The tight contact between α-Fe_2O_3 nanoparticles and the graphene sheets can be demonstrated by the fact that the α-Fe_2O_3 nanoparticles do not separate from the graphene sheets even after long time sonication. The integration of porous α-Fe_2O_3 nanoparticles possessing tunable crystallinity (or crystallite size) and pore size with crumpled graphene can reduce the diffusion path of ions, accommodate

DOI: 10.1021/am507910f
ACS Appl. Mater. Interfaces 2015, 7, 75−79

more electroactive species, and provide highly accessible surface area and excellent electrical conductivity in supercapacitors.[9,18]

The pore structure and the specific surface areas of S-PIGCs were further characterized by nitrogen adsorption/desorption measurement and analyzed using the Barrett−Joyner−Halenda (BJH) and Brunauer−Emmett−Teller (BET) methods. The typical IV isotherms with type H4 hysteresis loops (Figure 3a) confirm the formation of the slitlike pores,[22] generated from the local decomposition and the removal of water.[23] The average pore diameter was calculated to be 3.4 nm, based on the BJH plot (the inset of Figure 3a). This result is consistent with the TEM observation. The BET specific surface area and pore volume of the S-PIGCs are 95.9 $m^2\ g^{-1}$ and 0.29 $cm^3\ g^{-1}$, respectively, which are higher than those of RGO-FeOOH (61.7 $m^2\ g^{-1}$ and 0.25 $cm^3\ g^{-1}$) and R-PIGCs (51.1 $m^2\ g^{-1}$ and 0.23 $cm^3\ g^{-1}$) (see Figure S3 in the Supporting Information). The large surface area and pore volume are essential for the electrode materials to achieve large capacitance, because they could reduce ion transport limitation in electrodes and ensure full utilization of electrode materials.

The local structure of S-PIGCs was investigated by Raman analysis comparing with that of GO (Figure 3b). The two bands located at around 1338 and 1585 cm^{-1} correspond to the typical D and G band of GO, respectively. The Raman spectrum of S-PIGCs shows several characteristic peaks at 212, 275, 385, 485, and 579 cm^{-1} from α-Fe_2O_3, whereas the D and G peaks from graphene were also observed.[6] Also, the higher D/G intensity ratio of S-PIGCs than that of GO indicates that the formation of α-Fe_2O_3 nanoparticles on GO sheets leads to the disorderly stacking of the graphene sheets and significantly decreasing of the graphene layer numbers.[24] The thermogravimetric analysis (TGA) confirms the content of α-Fe_2O_3 in S-PIGCs (Figure S4 in the Supporting Information). It is found that the mass ratio of α-Fe_2O_3 is 81.6%.

Figure 4 shows the results of the electrochemical measurements tested using a three-electrode cell in 1 M Na_2SO_4 aqueous solution within a potential window from −0.3 to −1 V (vs Ag/AgCl). The cyclic voltammetry (CV) curves at various scan rates are shown in Figure 4a. The good reversibility behavior is testified by the nearly mirror-image current response in the CV curves. In addition, the S-PIGCs deliver an obvious pseudocapacitive characteristic, which can be attributed to the reduction/oxidation of Fe^{3+} and Fe^{2+}/Fe.[5] Figure 4b shows the charge−discharge (CD) curves of the S-PIGCs electrode at different current densities. The smooth sloping voltage profiles indicate a pseudocapacitive feature, consist with the CV results. The specific capacitance is calculated according to the discharge curves. Compared with R-PIGCs (227.9 F g^{-1}) (Figure 4c), the S-PIGCs achieve a higher specific capacitance of 343.7 F g^{-1} at a current density of 3 A g^{-1}, which is also higher than the recently reported values of other α-Fe_2O_3-based electrodes, such as mesoporous hematite nanostructures (116 F g^{-1}),[4] nanoscale iron oxide-carbon nanoarchitectures (84 F g^{-1}),[16] and α-Fe_2O_3 mesocrystals/graphene nanohybrid (306.9 F g^{-1}).[6] Furthermore, the S-PIGCs showed good rate performance with a capacitance of 182.1 F g^{-1} retained at a current density as high as 10 A g^{-1} (Figure 4d). Although the rate performance is lower than that of the R-PIGCs because of the limitation of H^+ and Na^+ ions diffusion and some inaccessible pores and voids at high current density, the specific capacitance is still very high at such high current density (Figure 4d). It is well-established that there is a trade-off between the electrical conductivity in the solid phase and the ionic transport in the pores.[1] The superior electrochemical properties of the S-PIGCs were further confirmed by the electrochemical impedance spectroscopy (EIS) (see Figure S5 in the Supporting Information). Obviously, excellent capacitive behavior can be obtained when RGO-FeOOH composites are annealed at a slow heating rate. This phenomenon might be attributed to the fact that S-PIGCs obtained at a slow heating rate possess higher open porosity, larger surface area, and appropriate crystallinity (or crystallite size).

The electrochemical stability of the S-PIGCs electrode was examined under continuous charge/discharge test at a current density of 10 A g^{-1} for 50 000 cycles (see Figure S6 in the Supporting Information). The capacitance retention of the S-PIGCs is 95.8% after 50,000 cycles, suggesting a long-term cycling stability of the S-PIGCs electrode. The high Columbic efficiency (~98.6%) of the S-PIGCs electrode indicates a highly reversibility of the electrode material (see Figure S7 in the Supporting Information). We postulate two factors in improving a long cycle life and a high reversibility for S-PIGCs electrode. First, the open porous in α-Fe_2O_3 nanoparticles effectively reduces the diffusion length of ions promoting fast Faradaic charging and discharging of α-Fe_2O_3 nanoparticles. Second, the graphene sheets serve as a conductive matrix, not only minimizing the aggregation of α-Fe_2O_3 nanoparticles but also maximizing the electrochemically accessible area and facilitating the charge-transfer process.

In summary, we have successfully synthesized porous α-Fe_2O_3-graphene composites (S-PIGCs) using a facile hydrothermal process followed by a slow annealing. The as-prepared material has a large specific surface area of 95.9 $m^2\ g^{-1}$. The ultrahigh capacitance of the composites results from the synergetic effect of optimally mesoporous crystalline nature of α-Fe_2O_3 and the crumpled structure of graphene sheets. The porous α-Fe_2O_3 facilitates electrolyte access to the electrochemical sites and ensures short ion diffusion path lengths, and the crumpled graphene sheets enhance the electrical conductivity of the whole electrode. The fantastic structure of the obtained S-PIGCs also holds the potential promise in other energy storage applications.

■ ASSOCIATED CONTENT

Ⓢ Supporting Information

Detailed preparation and characterization, and supplementary tables and figures. This material is available free of charge via the Internet at http://pubs.acs.org.

■ AUTHOR INFORMATION

Corresponding Authors

*E-mail: liangao@mail.sic.ac.cn. Fax: +86-21-52413122. Tel: +86-21-52412718.

*E-mail: songxfeng@sjtu.edu.cn.

Notes

The authors declare no competing financial interest.

■ ACKNOWLEDGMENTS

The authors greatly acknowledge the financial support by the National Natural Science Foundation of China (51302169), the Shanghai Municipal Natural Science Foundation (12ZR1414300), the SJTU-SMC Foundation for Excellent Young Scholar, and the Third Phase of 211 Project for Advanced Materials Science (WS3116205007).

DOI: 10.1021/am507910f
ACS Appl. Mater. Interfaces 2015, 7, 75−79

REFERENCES

(1) Wang, G.; Zhang, L.; Zhang, J. A Review of Electrode Materials for Electrochemical Supercapacitors. *Chem. Soc. Rev.* **2012**, *41*, 797−828.

(2) Xu, C.; Xu, B.; Gu, Y.; Xiong, Z.; Sun, J.; Zhao, X. Graphene-Based Electrodes for Electrochemical Energy Storage. *Energy Environ. Sci.* **2013**, *6*, 1388−1414.

(3) Wang, Y.; Xia, Y. Recent Progress in Supercapacitors: From Materials Design to System Construction. *Adv. Mater.* **2013**, *25*, 5336−5342.

(4) Wang, D.; Wang, Q.; Wang, T. Controlled Synthesis of Mesoporous Hematite Nanostructures and Their Application as Electrochemical Capacitor Electrodes. *Nanotechnology* **2011**, *22*, 135604.

(5) Lee, K.; Deng, S.; Fan, H.; Mhaisalkar, S.; Tan, H.; Tok, E.; Loh, K.; Chin, W.; Sow, C. α-Fe_2O_3 Nanotubes-Reduced Graphene Oxide Composites as Synergistic Electrochemical Capacitor Materials. *Nanoscale* **2012**, *4*, 2958−2961.

(6) Yang, S.; Song, X.; Zhang, P.; Sun, J.; Gao, L. Self-Assembled α-Fe_2O_3 Mesocrystals/Graphene Nanohybrid for Enhanced Electrochemical Capacitors. *Small* **2014**, *10*, 2270−2279.

(7) Pumera, M. Graphene-Based Nanomaterials for Energy Storage. *Energy Environ. Sci.* **2011**, *4*, 668−674.

(8) Jiang, J.; Li, Y.; Liu, J.; Huang, X.; Yuan, C.; Lou, X. W. D. Recent Advances in Metal Oxide-Based Electrode Architecture Design for Electrochemical Energy Storage. *Adv. Mater.* **2012**, *24*, 5166−5180.

(9) Xiong, S.; Yuan, C.; Zhang, X.; Xi, B.; Qian, Y. Controllable Synthesis of Mesoporous Co_3O_4 Nanostructures with Tunable Morphology for Application in Supercapacitors. *Chem.—Eur. J.* **2009**, *15*, 5320−5326.

(10) Zhang, G.; Lou, X. W. General Solution Growth of Mesoporous $NiCo_2O_4$ Nanosheets on Various Conductive Substrates as High-Performance Electrodes for Supercapacitors. *Adv. Mater.* **2013**, *25*, 976−979.

(11) Wang, R.; Yan, X.; Lang, J.; Zheng, Z.; Zhang, P. A Hybrid Supercapacitor Based on Flower-Like $Co(OH)_2$ and Urchin-Like VN Electrode Materials. *J. Mater. Chem. A* **2014**, *2*, 12724−12732.

(12) Ren, Y.; Ma, Z.; Bruce, P. G. Ordered Mesoporous Metal Oxides: Synthesis and Applications. *Chem. Soc. Rev.* **2012**, *41*, 4909−4927.

(13) Yang, P.; Zhao, D.; Margolese, D. I.; Chmelka, B. F.; Stucky, G. D. Generalized Syntheses of Large-Pore Mesoporous Metal Oxides with Semicrystalline Frameworks. *Nature* **1998**, *396*, 152−155.

(14) Lu, A. H.; Schüth, F. Nanocasting: A Versatile Strategy for Creating Nanostructured Porous Materials. *Adv. Mater.* **2006**, *18*, 1793−1805.

(15) Liu, J.; Xue, D. Thermal Oxidation Strategy Towards Porous Metal Oxide Hollow Architectures. *Adv. Mater.* **2008**, *20*, 2622−2627.

(16) Sassin, M. B.; Mansour, A. N.; Pettigrew, K. A.; Rolison, D. R.; Long, J. W. Electroless Deposition of Conformal Nanoscale Iron Oxide on Carbon Nanoarchitectures for Electrochemical Charge Storage. *ACS Nano* **2010**, *4*, 4505−4514.

(17) Brezesinski, T.; Wang, J.; Tolbert, S. H.; Dunn, B. Ordered Mesoporous α-MoO_3 with Iso-Oriented Nanocrystalline Walls for Thin-Film Pseudocapacitors. *Nat. Mater.* **2010**, *9*, 146−151.

(18) Lou, X. W.; Deng, D.; Lee, J. Y.; Archer, L. A. Thermal Formation of Mesoporous Single-Crystal Co_3O_4 Nano-Needles and Their Lithium Storage Properties. *J. Mater. Chem.* **2008**, *18*, 4397−4401.

(19) Zhu, X.; Zhu, Y.; Murali, S.; Stoller, M. D.; Ruoff, R. S. Nanostructured Reduced Graphene Oxide/Fe_2O_3 Composite as a High-Performance Anode Material for Lithium Ion Batteries. *ACS Nano* **2011**, *5*, 3333−3338.

(20) Yang, S.; Song, X.; Zhang, P.; Gao, L. Crumpled Nitrogen-Doped Graphene-Ultrafine Mn_3O_4 Nanohybrids and Their Application in Supercapacitors. *J. Mater. Chem. A* **2013**, *1*, 14162−14169.

(21) Wen, Z.; Wang, X.; Mao, S.; Bo, Z.; Kim, H.; Cui, S.; Lu, G.; Feng, X.; Chen, J. Crumpled Nitrogen-Doped Graphene Nanosheets with Ultrahigh Pore Volume for High-Performance Supercapacitor. *Adv. Mater.* **2012**, *24*, 5610−5616.

(22) Gu, D.; Lu, Y.; Yang, B. Facile Preparation of Micro-Mesoporous Carbon-Doped TiO_2 Photocatalysts with Anatase Crystalline Walls under Template-Free Condition. *Chem. Commun.* **2008**, 2453−2455.

(23) Wang, Y.; Cao, J.; Wang, S.; Guo, X.; Zhang, J.; Xia, H.; Zhang, S.; Wu, S. Facile Synthesis of Porous α-Fe_2O_3 Nanorods and Their Application in Ethanol Sensors. *J. Phys. Chem. C* **2008**, *112*, 17804−17808.

(24) Li, L.; Guo, Z.; Du, A.; Liu, H. Rapid Microwave-Assisted Synthesis of Mn_3O_4-Graphene Nanocomposite and Its Lithium Storage Properties. *J. Mater. Chem.* **2012**, *22*, 3600−3605.

DOI: 10.1021/am507910f
ACS Appl. Mater. Interfaces 2015, 7, 75−79